Proton radiography as an electromagnetic field and density perturbation diagnostic (invited)

Mackinnon, A. J., Patel, P. K., Town, R. P., Edwards, M. J., Phillips, T., Lerner, S. C., Price, D. W., Hicks, D., Key, M. H., Hatchett, S., Wilks, S. C., Borghesi, M., Romagnani, L., Kar, S., Toncian, T., Pretzler, G., Willi, O., Koenig, M., Martinolli, E., ... Boehly, T. (2004). Proton radiography as an electromagnetic field and density perturbation diagnostic (invited). *Review of Scientific Instruments*, *75*(10), [3531]. https://doi.org/10.1063/1.1788893

Published in:
Review of Scientific Instruments

Document Version:
Publisher's PDF, also known as Version of record

Proton radiography as an electromagnetic field and density perturbation diagnostic (invited)

A. J. Mackinnon, P. K. Patel, R. P. Town, M. J. Edwards, T. Phillips et al.

Citation: Rev. Sci. Instrum. **75**, 3531 (2004); doi: 10.1063/1.1788893
View online: http://dx.doi.org/10.1063/1.1788893
View Table of Contents: http://rsi.aip.org/resource/1/RSINAK/v75/i10
Published by the American Institute of Physics.

Proton radiography as an electromagnetic field and density perturbation diagnostic (invited)

A. J. Mackinnon,[a] P. K. Patel, R. P. Town, M. J. Edwards, T. Phillips, S. C. Lerner, D. W. Price, D. Hicks, M. H. Key, S. Hatchett, and S. C. Wilks
Lawrence Livermore National Laboratory, P. O. Box 808, L-399 Livermore, California 94550

M. Borghesi, L. Romagnani, and S. Kar
Department of Physics, Queens University, Belfast, United Kingdom

T. Toncian, G. Pretzler, and O. Willi
Heinrich University, Dusseldorf, Germany

M. Koenig, E. Martinolli, S. Lepape, A. Benuzzi-Mounaix, and P. Audebert
Ecole Polytechnique, France

J. C. Gauthier
CEA, Bruyere, Bordeaux, France

J. King, R. Snavely, and R. R. Freeman
University of California, Davis, California

T. Boehlly
Laboratory for Laser Energetics, Rochester, New York

(Presented on 19 April 2004; published 5 October 2004)

Laser driven proton beams have been used to diagnose transient fields and density perturbations in laser produced plasmas. Grid deflectometry techniques have been applied to proton radiography to obtain precise measurements of proton beam angles caused by electromagnetic fields in laser produced plasmas. Application of proton radiography to laser driven implosions has demonstrated that density conditions in compressed media can be diagnosed with million electron volt protons. This data has shown that proton radiography can provide unique insight into transient electromagnetic fields in super critical density plasmas and provide a density perturbation diagnostics in compressed matter. © *2004 American Institute of Physics.*
[DOI: 10.1063/1.1788893]

I. INTRODUCTION

The generation of multimillion electron volts proton and ion beams in high intensity interactions of ultra-short laser pulses with solid targets is a rapidly growing research area. Distinctly collimated beams with cut-off energies in excess of 50 meV have been observed at high laser intensity.[11] The remarkable collimation, small transverse emittance, high cut-off energy, and emission from the unirradiated rear of the target distinguish these beams from less directed, lower energy protons observed in earlier work at lower laser intensity.[2,3] Another very important feature of these protons is that they are emitted in a timescale similar to the laser pulse duration, which is typically in the range of a few hundred femtoseconds to a few picoseconds. These properties make laser driven proton beams a unique probing tool for diagnosing electric and magnetic fields and density homogeneity in highly transient plasmas and shocked materials. In fact these proton beams have recently been used as a probe beam to investigate electromagnetic fields in plasmas.[4] In these pioneering experiments the proton beam was used as a point projection source to backlight the fields produced by the interaction of a separate laser with a solid target. Deflections in the proton backlighter were recorded from observations of localized increase in proton signal in particular areas on the spatially resolving particle detector.[5] This article reports on the development of (i) grid deflectometry techniques with proton beams for electromagnetic field diagnostics, (ii) the use of protons to diagnose density perturbations in dense plasmas, and (iii) proton imaging of shock induced plasmas effects.

II. GRID DEFLECTOMETRY USING PROTONS

Moire deflectometry is a widely used optic technique in to diagnose refractive index gradients[6] and strain in optical components.[7,8] Moiré effects have also been used in electron microscopy to diagnose dislocations in metals,[9] and the effect has recently been demonstrated with laser driven proton beams on the JanUSP laser at Lawrence Livermore National Laboratory (Livermore, CA).[10,11] In optics single grid refractometry methods have also been used in conjunction with x-ray lasers to measure density gradients in laser produced plasma.[12] We will describe experiments which have utilized the development of single grid deflectometry as a technique to quantitatively measure proton deflections from electro-

[a]Electronic mail: mackinnon2@LLNL.GOV

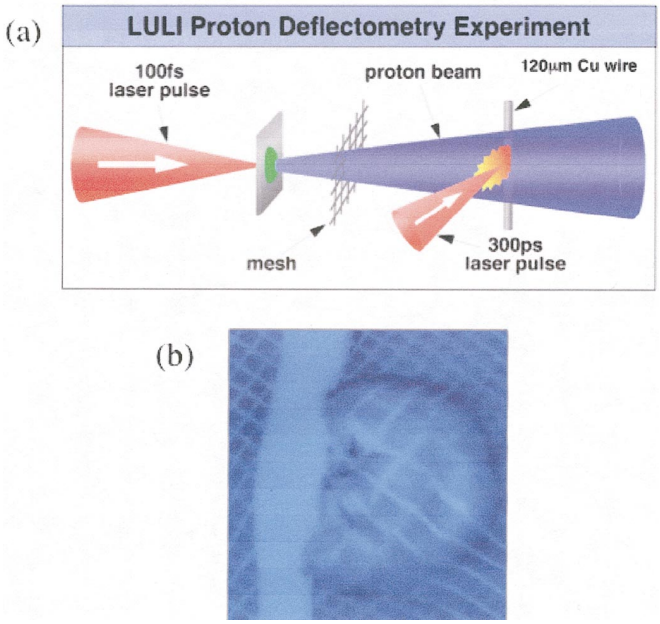

FIG. 1. (Color) (a) Schematic of deflectometry experiment undertaken on the LULI laser at Ecole Polytechnique, France. The interaction beam creates a plasma which is then probed by protons created by a second femtosecond laser pulse focused onto a surrogate target. The proton beam is broken up into hundreds of small beamlets as it passes through a 1500 lpi mesh before traversing the plasma. (b) 7 MeV Proton image showing distortions of the mesh as the protons pass through the plasma region.

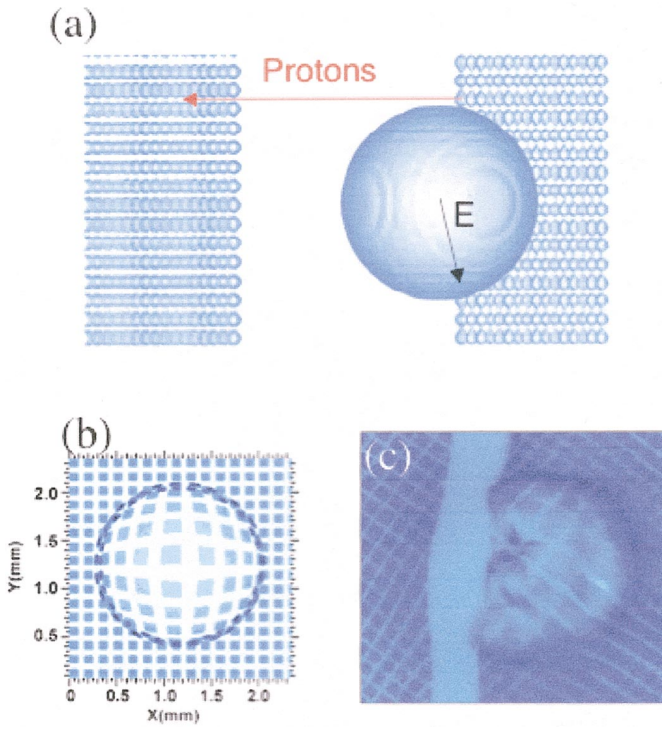

FIG. 2. (Color) Hybrid PIC code simulations of protons traversing a spherically symmetric region containing a radial electric field. (a) Geometry of the simulation, the region has the same transverse dimensions as the experimental plasma and the relative positions of the proton source and detector match the experiment. (b) Simulated Image on film pack. The distortions in the mesh closely match the experimental data shown in (c), in terms of the radially symmetric increase in effective magnification of the mesh elements inside the plasma, the pile up in proton signal at the outer edges of the plasma, and the barrel type distortion of the mesh elements inside the plasma. (c) Experimental data.

magnetic fields driven in laser produced plasmas.[13] This experiment was carried out on the femtosecond LULI laser at Ecole Polytechnique, France, Fig. 1(a) shows a schematic of the experimental arrangement. In this experiment a 300 ps duration interaction beam with 1 mm wavelength and 50 J energy was focused at an irradiance of 5×1015 W cm-2 onto the surface of a 125 μm tungsten wire target. The fields produced during this interaction were diagnosed by passing a million electron volt protons through the plasma region at 90° to the interaction beam onto a multilayer film pack (side-on imaging). The proton beam was produced by focusing a 20 J pulse, of duration 300 fs and 1.054 μm wavelength at a solid tungsten target at an irradiance of 1×10^{19} W cm^{-2}. Protons, which were accelerated from contaminants on the rear surface of the target passed through a grid before passing through the interaction plasma. By tracking the deviations of these grid elements small angular proton beam deflections can be quantitatively evaluated. Comparison of these deflections with simple proton ray tracing models allows the field structure to be extracted from the deflectograms.

Figure 1(b) shows a proton deflectogram obtained from 10 MeV protons passing through the plasma, 150 ps before the peak of the interaction pulse. The laser is incident from the right and the plasma is the semispherical object roughly 200 μm in diameter in the center of the image. Electromagnetic fields inside the plasma have deflected the protons in a radially symmetric manner, away from the center of the plasma. These deflections lead to apparent enlargement of the periodicity of the mesh, by roughly a factor of two. In essence the plasma is acting like a negative lens by providing a magnified image of the mesh. Another striking feature of this image is the large pile up in proton signal just on the outer boundary of the plasma. These features are both consistent with a radial electric field deflecting protons away from the center of the plasma, as will be shown in the next section.

III. (LSP) AND LASNEX SIMULATIONS

The experimental images were interpreted with the aid of two-dimensional (2D) Lasnex hydrocode[14] and (LSP) hybrid fluid-(PIC) code simulations.[15] Lasnex was used to model the evolution of the plasma density and temperature conditions with self consistent B fields while LSP was used to trace the proton beam through the plasma to post process the electric and magnetic field profiles to compare directly with the experimental images. The utility of proton ray tracing as an interpretation tool for deflectometry was tested using an analytic electric field geometry. Figure 2(a) shows a schematic of a LSP simulation of a point source of 7 MeV protons propagating through a spherically symmetric region containing a radial E field with constant magnitude of 1×10^{9} Vm^{-1} and with the same transverse dimension as in the experiment. After traversing through this simulated plasma region, the protons were transported to a film pack 5 cm away-as in the experiment. A simulated image at the film pack, shown in Fig. 2(b), closely reproduces the data with both the pile-up effect of protons at the edge of the

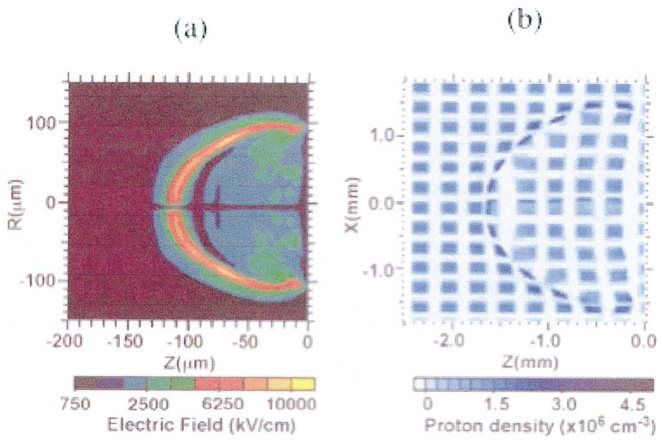

FIG. 3. (Color) Lasnex and LSP simulations of the experimental parameters. (a) Radial electric fields calculated from the radial pressure gradient term obtained from Lasnex simulations of the deflectometry experiment. (b) Proton density plot at the image plane from hybrid LSP code proton trajectories of 7 MeV protons that have traversed the Lasnex calculated electric fields.

plasma and the same apparent increase in the mesh element size inside the plasma (another feature common to both the data and the simulations is the barrel distortion of the mesh inside the plasma).

Electric field contours from a Lasnex simulation of a plasma generated by focusing a laser pulse with the experimental parameters onto a thick slab target is shown in Fig. 3(a). In this simulation the electric field is driven by gradients in the plasma pressure as the plasma expands radially. For the conditions of the experiment, radial fields in the range of $5-10\times10^{8}$ Vm^{-1} are generated by these plasmas. LSP simulations of proton deflectometry through this field distribution produces deflections that are in good qualitative agreement with the experimental data, in particular the enhanced proton signal at the plasma edge and increase in effective magnification of the mesh inside the plasma. In terms of absolute terms the deflection observed from the simulations is around a factor of two less than that in the experiment, this in turn corresponds approximately to a factor of two reduction in the observed electric field. This discrepancy may be due to the absence of suprathermal electrons in the simulation, which would be expected to generate large electric fields compared to purely thermal plasma expansion. These simulations also showed that due to the symmetry of the torroidal B field there is no contribution to the observed deflections this geometry (in effect the deflections cancel over the line of sight of the proton probe). These issues will be discussed in more detail in a forthcoming publication.

IV. PROTON RADIOGRAPHY OF DENSITY PERTURBATIONS

Due to their large range, million electron volts protons are also particularly suitable for radiographic applications of dense plasmas and solid materials. In particular and multimillion electron volts proton beams with low emittance and short pulse length can be used to dynamically probe shocked and compressed material with high temporal and spatial resolution. For example, 30–50 MeV protons produced by a (PW)laser would be sufficiently energetic to probe cold, compressed (NIF) cores. Multiple scattering imposes strong influences of the imaging properties of these proton beams and in some cases limits the achievable resolution. An experiment to investigate proton probing of a laser driven implosion was carried out on the 100TW Vulcan laser system to investigate the suitability of proton radiography to diagnose overdense plasmas. As shown in Fig. 4(a), six beams of Vulcan (each 1 μm wavelength, 1 ns duration) were focused onto a microballoon at an irradiance of 1×10^{13} W cm^{-2} and without phase plates. The individual beam energy was in the range of 100–150 J giving a maximum energy on target of 900 J. The targets were plastic mi-

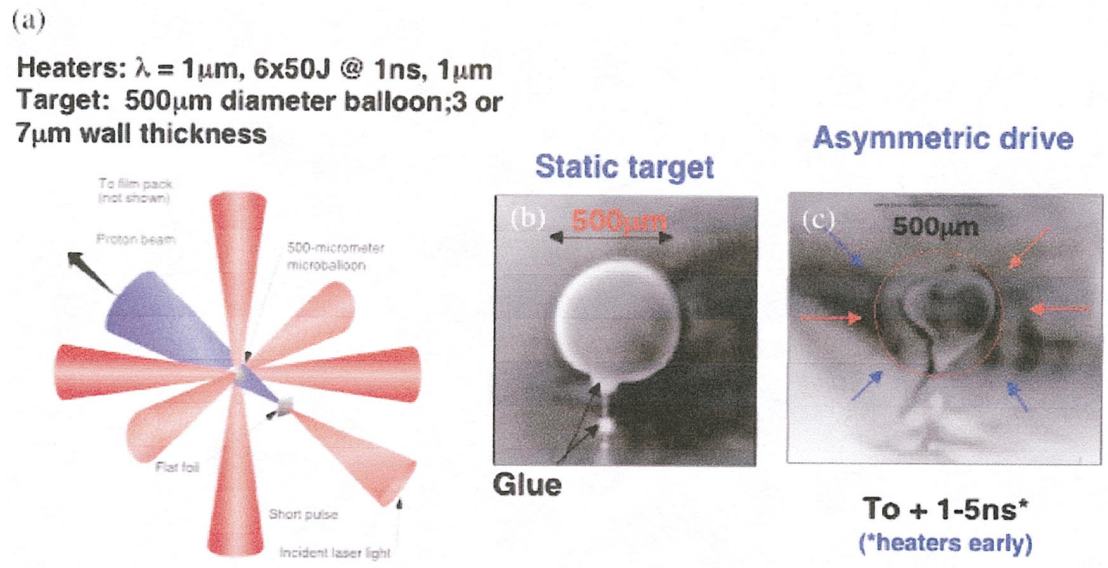

FIG. 4. (Color) Proton radiography of laser driven implosions. (a) The implosion and backlighting geometry. Six beams of the Vulcan laser at Rutherford Appleton laboratory were used to drive an implosion of 500 mm microballoons. Proton radiography was used to diagnose the temporal evolution of the implosion. (b) Proton radiograph in 7 MeV protons of a cold microballoon. (c) Proton radiograph of an asymmetric implosion. Timing differences in three of the heater beams have caused strong density non uniformities to develop.

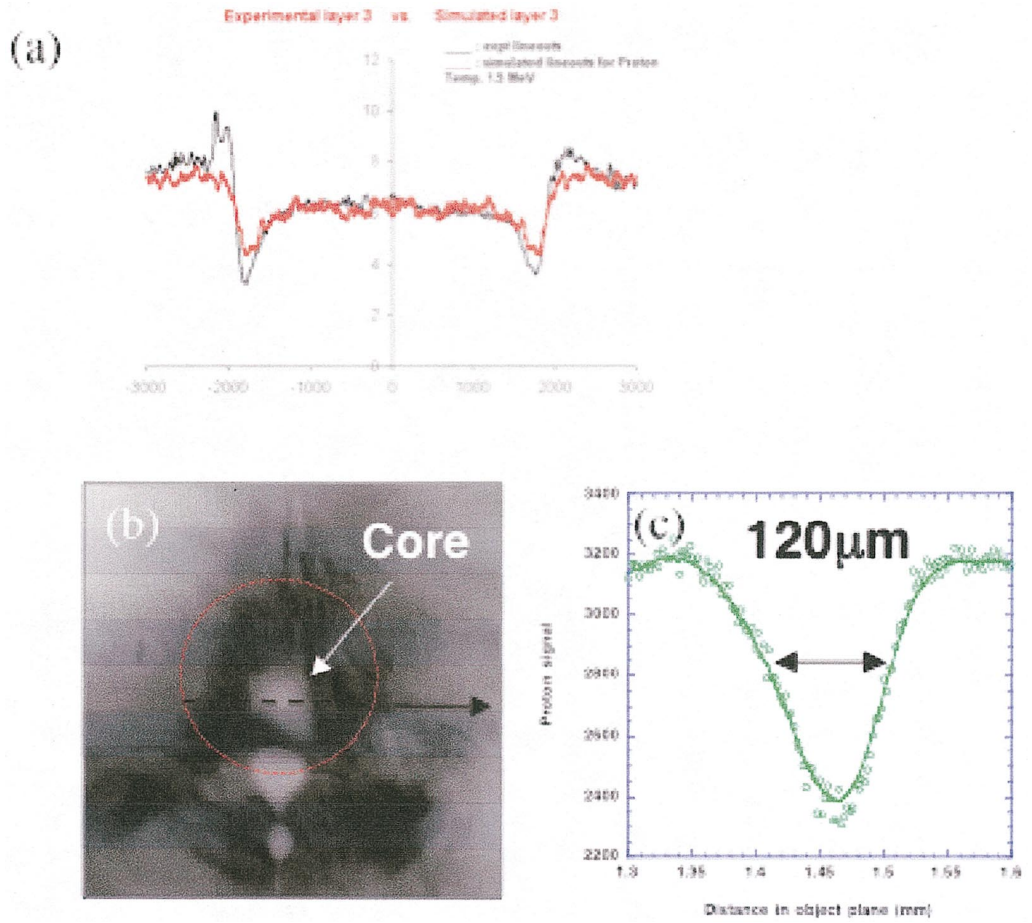

FIG. 5. (Color) (a) Lineout of proton dose through the cold shell plus Monte Carlo simulations based on SRIM calculations. (b) 7 MeV Proton radiograph of a compressed shell close to stagnation. (c) Lineout through dense core region.

croballoons (CD_2), 500 μm in diameter and with two different wall thickness: 3 and 7 μm. The heater beams were arranged such that they illuminated the target tangentially from six orthogonal directions, giving the best symmetry this implosion.

The implosion was diagnosed by laser produced protons in the million electron volts range obtained by focusing a 50–100 J chirped pulse amplification (CPA) laser pulse, duration 1 ps onto a solid tungsten foil at an irradiance of 5×10^{19} W cm^{-2}. Synchronization of the 1 ns heater beams to the picosecond backlighter beam was measured to within 100 ps using an optical streak camera. Million electron volts protons were obtained from a 25 μm tungsten foil and the proton beam was characterized by an exponential spectrum of mean temperature 3 MeV and a high-energy cut-off around 15–20 MeV.[1] The detector consisted of a multilayer pack containing spatially resolving dosimetry film (RCF) and particle track detectors (CR-39) as described previously. This arrangement gave a diagnostic in which each layer was filtered by the preceding layer, giving a series of images on each shot each with a slightly different energy, ranging from 3 to 15 MeV. Experimentally it was found that little or no protons were produced on shots when the back surface of the proton target was exposed to the coronal plasma surrounding the imploding balloon. To overcome this a 6 μm aluminum foil was used to shield the proton foil from the hot coronal plasma produced during the implosion. This observation is consistent with the formation of a preformed plasma on the rear of the proton target before the arrival of the CPA laser pulse. Such a plasma at the rear surface of the target can reduce the accelerating electric field and disrupts the proton acceleration mechanism.[5] The aluminum prefoil protected the back surface of the proton backlighter foil from scattered or specularly reflected light from the heater beams and low energy x-rays or fast ions from the implosion plasma and thus prevented the formation of a preplasma which would degrade the proton beam. A proton radiograph in 7 MeV protons, of a cold (undriven) microballoon is shown in Fig. 4(b). The balloon has good contrast and the shell is well resolved. Analysis of the sharpness of the edges of the balloon gives resolution ~7–10 μm for this proton energy. The main limitation on the resolution in this experiment is actually due to scattering in the target rather than intrinsic emittance of the proton source. As shown in Fig. 5(a) the balloon impresses a 50% modulation onto the proton beam with a characteristic shape where the proton signal first reduces below the background then overshoots just outside the shell. This behavior is consistent with multiple small angle scattering of the protons as they go through the microballon wall. Also shown in Fig. 5(a) proton Monte Carlo simulations of a point source propagating through the microballon using 7 MeV protons. It can be seen that these simulations agree

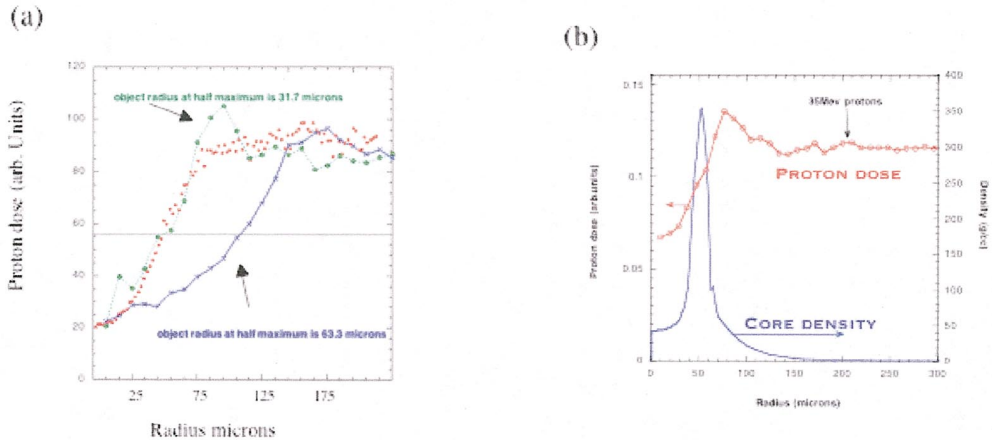

FIG. 6. (Color) (a) Lineout of core region from data shown in Fig. 5(b) (small circles) and Monte Carlo simulations of a spherically symmetric core with a Gaussian density profile with the same peak density of 3 g/cc but two different core diameters; 62 μm (circles with dashed line) and 126 μm (crosses with full line). The best fit to the data is obtained with the 62 μm core diameter. (b) 1D Monte Carlo simulation of proton radiograph through a density profile generated from 1D hydrocode, (hydra) of a mistimed NIF shot which just failed to reach ignition point.

well with the data, reproducing the shape of the edge of the balloon and confirming that multiple scattering is responsible for modulating the proton beam and forming the image of the balloon.

The evolution of the capsule density profile during the implosion was studied by varying the delay between the backlighter and the implosion beams. Figure 4(c) shows a proton image of a capsule where the drive was very asymmetrical due to significant timing difference between some of the drive beams. In this case the laser beams on the left-hand side of the image arrived between 1 and 2 ns before the laser beams on the right-hand side. This led to the significant distortions with the shell traveling much further inward on the left compared to the right. With more symmetrical drive conditions the capsule remains roughly spherical as the implosion proceeds.

Proton radiographs of shell as the implosion proceeded towards stagnation (at T_o+3 ns for this 3 μm wall thickness shell), are shown in the radiograph in Fig. 5(c). Even though free from the gross asymmetries observed in the implosion of Fig. 4(c), it is clear that the implosion still suffers from significant asymmetric drive conditions. At this time the shell has assembled to peak density with a full width half maximum (FWHM) of 120 μm. The stagnated shell has formed in the lower third of the original shell, consistent with higher drive energy from the upper beams, and is not spherical. Proton radiography clearly resolves the core asymmetry and allows the shape of density profile to be inferred. In order to obtain an estimate of the density profile in the core, Monte Carlo simulations of a Gaussian shaped density featured were carried out. Figure 6(a) shows a line-out across the minor diameter of the core feature, together with the output from a Monte Carlo simulation. The peak density of the core and the radius (FWHM) of the function were treated as variable parameters until the best match with the data was obtained. A profile with a peak density of 3 g/cc and FWHM diameter of 62 μm gave good agreement with the data, as shown in Fig. 6(a). It is clear that at this proton energy there is considerable blurring of the core, this is due to scattering of these relatively low energy protons as they traverse the core. From the simulations the blurring was negligible for higher energy protons ($>$12 MeV) and shows that the technique produces high resolution images of density profiles if protons of high enough energy can be produced.

The feasibility of proton radiography for diagnosing density uniformity in very dense objects such as a compressed inertial confinement fusion shell was tested by applying our Monte Carlo model to a one-dimensional (1D) hydra simulation of a NIF implosion. The most important area where proton radiography could provide new or complimentary information to a fusion diagnostic such as neutron imaging is for an implosion that does not quite reach ignition. This implosion may not produce enough neutrons to provide a high fidelity image of the shape of the core region and so other diagnostics must be developed which can characterize the spatial nonuniformity that prevented ignition from occurring. The density conditions in a nonigniting core can still be extreme, with peak densities in the core of around 350 g/cc and so one obvious candidate for this diagnostic is high energy x-ray radiography in the 20–40 keV energy range. However developing x-ray techniques with the required flux and micron scale resolution is not trivial and is an ongoing research and development effort in many laboratories.[16] Protons with energy in the 30–50 MeV range could also probe cores with these densities. Figure 6(b) shows a hydra profile of a "failed" indirect drive NIF implosion, where some of the shocks used to assemble the high density fuel have been mistimed. The resulting profile is typical of a stagnating imploded shell with a high density shell surrounding a hollow core. In this particular case the shell density peaks at 350 g/cc at a radius of 50 μm surrounding a core region with density around 50 g/cc. A point projection proton image of the object in 35 MeV protons is shown in Fig. 6(b). The full width half maximum of the dip in the proton dose is closely correlated with the location of the peak density thus showing the promise of this technique. In a real implosion other factors such as pressure gradient electric fields and hot plasma effects on the proton propagation will also contribute to the proton dose observed on the

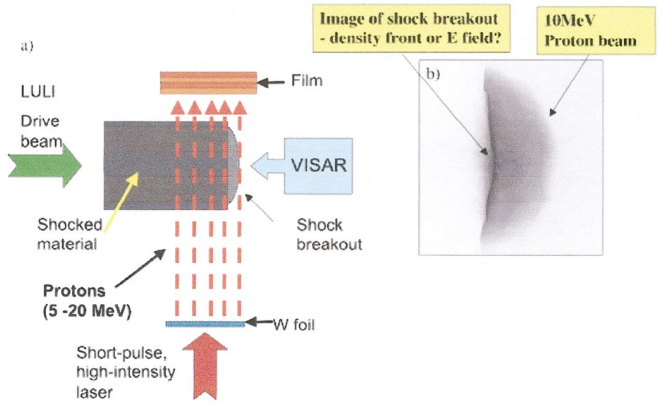

FIG. 7. (Color) (a) Schematic of proton radiograph experiment to diagnose the plasma produced by a shock breaking out of the back of an aluminum pusher. (b) Proton radiograph of the plasma produced 7 ns after the shock began propagating through a 15 μm aluminum foil.

detector. Electric field effects would lead to a general deflection rather than scattering shown here. In fact the deflectometry techniques could be used to diagnose these fields thus providing additional information on pressure gradients in the core of an inertial confinement fusion target. Future work will also include a model that includes the effects of proton propagation through a hot plasma, which will tend to reduce the amount of scattering at a given proton energy.

V. PROTON RADIOGRAPHY OF SHOCK FRONTS

One very important application of proton radiography is the measurement of shock fronts inside opaque materials or at the plasma vacuum interface created when a shock wave breaks out from a solid surface. Point projection proton radiography was used to investigate the density profile generated at the rear surface of a laser heated foil. The laser driving the shock in this case was part of the LULI laser; 70 J pulse, 500 ps in duration and focused to a spot size of 400 μm giving an irradiance around 5×10^{13} W cm^{-2}. The protons were produce by the LULI short pulse duration beam as described in Sec. I and shown schematically in Fig. 7(a). A 10 MeV proton radiograph of a shock breaking out of the rear of an aluminum target is shown in Fig. 7(b). This radiograph, taken 7 ns after the onset of the drive pulse at the front of the target, exhibits a striking increase in proton signal at the front of the plasma produced by the shock breakout. Shock propagation through the target was diagnosed with Visar interferometry and modeled using 1D hydrodynamic codes.[17] Monte Carlo simulations of proton propagation through hydrocode simulations of density profiles in the shock break out region cannot reproduce the proton signal enhancement at the vacuum plasma boundary. An electric field at the leading edge of the plasma is one possible source for this feature but it is unlikely that a field large enough to deflect 10 MeV protons could be driven by this low (few electron volts) temperature plasma and so the most probable mechanism for this observation is a density profile modification caused by a phase change in the expanding plasma. More detailed 2D simulations and experiments are underway to investigate these observations. Proton radiography of shock heated material is providing fundamental information on the density profile of a plasma expanding into vacuum which may be able to test theoretical models in this area.

ACKNOWLEDGMENT

This work was funded under the auspices of the U.S. Department of Energy by the Lawrence Livermore National Laboratory under Contract No. W-7405-ENF-48.

[1] S. P. Hatchett *et al.*, Phys. Plasmas **7**, 2076 (2000); R. A. Snavely *et al.*, Phys. Rev. Lett. **85**, 2945 (2000);E. L. Clark *et al.*, *ibid.* **84**, 670 (2000); A. Maksimchuk *et al.*, *ibid.* **84**, 4108 (2000); K. Nemoto *et al.*, Appl. Phys. Lett. **78**, 595-597 (2001); Y. Murakami, *et al.*, Phys. Plasmas **8**, 4138 (2001).
[2] S. J. Gitomer, Phys. Fluids **29**, 2679 (1986); A. P. Fews, *et al.*, Phys. Rev. Lett. **73**, 1801 (1994); F. N. Beg *et al.*, Phys. Plasmas **4**, 447 (1997).
[3] J. E. Crow, P. L. Auer, and J. E. Allen, J. Plasma Phys. **14**, 65 (1975); J. Denavit, Phys. Fluids **22**, 1385 (1979); Y. Kichimoto, *et al.*, Phys. Fluids **26**, 2308 (1983).
[4] M. Borghesi *et al.*, Plasma Phys. Controlled Fusion **43**, 267 (2001).
[5] M. Borghesi *et al.*, Phys. Plasmas **9** 3655 (2002).
[6] O. Kafri, Opt. Lett. **5**, 555 (1980); O. Kafri and I. Glatt, Opt. Eng. **24**, 944 (1985).
[7] O. Kafri and I. Glatt, *The Physics of Moiré Metrology* (Wiley, New York, 1990), and references therein.
[8] P. Theocaris and Moiré Fringes *Strain Analysis* (Permagon Press, Oxford, 1969).
[9] D. W. Pashley, J. W. Menter, and G. A. Basset, Nature (London) (London) **179**, 752 (1957).
[10] A. J. Mackinnon *et al.*, Appl. Phys. Lett. **82**, 3188 (2003).
[11] A. J. Mackinnon *et al.*, Rev. Sci. Instrum. **74**, 1917 (2003).
[12] K. Takahashi, R. Kodama, K. A. Tanaka, *et al.*, Phys. Rev. Lett. **84**, 2405 (2000).
[13] G. Pretzler *et al.*, (unpublished).
[14] G. B. Zimmerman and W. B. Kruer, Comments Plasma Phys. Controlled Fusion **2**, 51 (1975).
[15] D. R. Welch *et al.*, Nucl. Instrum. Methods Phys. Res. A **464**, 134 (2001).
[16] J. A. Koch *et al.*, Appl. Opt. **37**(10), 1784 (1998).
[17] M. Koening *et al.*, (unpublished).